



Semnan University

Mechanics of Advanced Composite Structures

journal homepage: <http://MACS.journals.semnan.ac.ir>

Active Vibration Control of Laminated Composite Beam Operating in Thermal Environment using PZT-5H Patches

K. Saini, A. Ravi Kiran, V. Kallannavar, S. Kattimani*

Department of Mechanical Engineering, National Institute of Technology Karnataka, Surathkal-575025, India

KEYWORDS

Active vibration control;
Effect of temperature;
PID Controller;
Laminated composite beam;
PZT actuators.

ABSTRACT

This paper investigates the influence of temperature on the active vibration control of laminated composite cantilever beams using collocative experimental and simulation techniques. The system identification toolbox of the MATLAB simulation tool is utilized to obtain the transfer function of the plant model. The adequate vibration attenuation of the glass-epoxy cantilever beam operating in various thermal environments is achieved using the proportional (P) and proportional-integral-derivative (PID) controllers. The vibration attenuation characteristics of the developed control algorithms are comprehensively investigated for a wide temperature range of $-20\text{ }^{\circ}\text{C}$ to $60\text{ }^{\circ}\text{C}$ using PZT-5H patches. Particular emphasis is given to the vibration control of the fundamental natural frequency of the laminated composite cantilever beam. The obtained results of open and closed-loop models are presented in both time and frequency domains. The results indicate that for all the temperatures considered, the PID controller is found to be more effective in vibration attenuation than the P controller. The vibration attenuation performance of the cantilever beam considerably improved at the higher magnitude of temperature values. The natural frequency of the system is reduced continuously with an increase in temperature.

1. Introduction

Composite materials are elementary structural materials comprising two or more constituent materials that are non-soluble in each other [1]. Composite materials are being extensively used in the prominent fields of engineering due to their superior fatigue life, durability, corrosion resistance, strength-to-weight ratio, etc. Properties such as high specific strength, specific modulus, creep, and thermal resistance allows the composite materials to be used in aviation, spacecraft, automotive, biomedical, and civil engineering applications. These materials are often expected to work effectively in challenging working environments such as moisture, high operating temperature, chemical environment, electric and magnetic fields, etc. The abrupt change in the working environment may adversely affect the functionality of the structural components [2,3].

In the past few decades, many researchers have investigated the influence of various environmental conditions on the mechanical

behavior of laminated composite structures. The works pertaining to vibration control of the laminated structures are also available in abundance. The self-monitoring and self-control capabilities of composite structures can be achieved by directly mounting the piezo-sensors and actuators [4]. Biswal et al. [5] performed an experimental and numerical investigation to understand the influence of the hygrothermal environment on the free vibration performance of the glass-epoxy laminated composite shells. Panda et al. [6] extended the work to study the effect of temperature and moisture on the vibration characteristics of delaminated woven glass-epoxy composite plates. The delaminated composite plates were prepared by embedding the teflon films between the layers of woven fiber composite mats. Fazeli et al. [7] developed an analytical closed-form solution to investigate the modal characteristics of laminated stepped beams using first-order shear deformation theory (FSDT), and analytical model results were validated with the experimental vibration

* Corresponding author. Tel: +91-9481413661
E-mail address: subhaskatti@nitk.edu.in

outcomes. They were considered a carbon-fiber/polyetheretherketone (PEEK) cantilever beam integrated with the piezoelectric actuation patch. Parameswaran et al. [8] achieved active vibration control (AVC) of a metallic cantilever beam using a lead zirconate-titanate (PZT) sensor and actuator pair. The results indicated that the vibration control is to be performed on the real-time operating system (RTOS) to avoid inconsistent transients.

Rimašauskienė et al. [9] experimentally investigated a cantilever composite beam's passive and active vibration regulator characteristics. The permanent cuboidal magnets were utilized to achieve the passive vibration control (PVC), and the macro fiber composite (MFC) patches were used to attain AVC. Li et al. [10] used PID negative feedback control algorithm to achieve active control of noise and vibration of the vibroacoustic cavity of an airplane. The parameters of the PID controller were optimized with an iterative method, and the optimization study was also performed to effective actuator patch placement. Additionally, the results obtained from the numerical model were compared with the experimental outcomes. Zhang et al. [11] used FSDT to develop an electromechanical coupled finite element (FE) model to investigate the vibration attenuation characteristics of the laminated composite plate. The PID controller and the linear quadratic regulator (LQR) controller algorithms were used for the investigation. Simonović et al. [12] investigated the AVC characteristics of the aluminum plate integrated with the strain gauge sensors and the piezoelectric actuators using a modified PID control algorithm. The fuzzy optimization method was used to discover the ideal orientation of the piezoelectric actuator patch. The PIC32MX440F256H microcontroller platform was utilized to implement the developed control algorithm to achieve more than 90% vibration suppression. Parameswaran et al. [13,14] performed the real-time AVC of the cantilever beam using a dedicated field-programmable gate array (FPGA) controller operating on the RTOS module. It was reported that the RTOS platform integrated with the FPGA module provides superior vibration attenuation in comparison with the general-purpose operating system (GPOS) platforms. The voltage feedback and the error feedback control strategy were examined for the vibration control of the smart cantilever beam.

Kamel et al. [15] proposed a new dynamic FE model for smart flexible beam vibration control. Advanced controlled algorithms such as PID, autotuning PID, self-tuning fuzzy controller, and proportional-derivative controller-based fuzzy controllers were adopted for the study. Sharma et

al. [16–18] utilized both numerical and experimental techniques to investigate the influence of temperature on the AVC performance of the smart cantilever beam mounted with the piezoelectric sensor and actuators. The multi-input single-output (MISO) technique was utilized to design a fuzzy logic controller for effective vibration attenuation. It was reported that the performance of the AVC strategy adopted was more efficient in elevated thermal environments. It was also noted that with the continual increment in the temperature magnitude, the structure's natural frequency reduces considerably. Kallannavar et al. [3] investigated the influence of temperature on the performance of the active constrained layer damping of the laminated composite sandwich plate. The face sheets of graphite-epoxy and the core of carbon nanotube-reinforced composites were considered for the study. It was reported that the vibration attenuation performance increases considerably with an increase in temperature. Gupta et al. [19] investigated the influence of temperature on the vibration attenuation characteristics of metal strips embedded with the PZT patches. The numerical model was developed based on the negative velocity feedback algorithm, and the experimental results suggest that the damping performance of the structure increases with the increase in temperature. Mohammadrezazadeh and Jafari [20–26] carried out extensive work on active vibration control of laminated composite structures such as rotating cylindrical shells, truncated conical shells, etc.

A comprehensive literature survey shows that the articles pertaining to the AVC of the laminated composite structures using numerical and analytical techniques are in abundance. However, experimental works to investigate the influence of temperature on the AVC of the laminated composite structures are scarce. Hence, in this article following novel attempts are made,

- A collective experimental and analytical outlook is planned to achieve the AVC of glass-epoxy composite cantilever beam operating in an elevated thermal environment (including sub-ambient temperatures).
- The vibration attenuation of laminated composite beam operating in a wide temperature range of $-20\text{ }^{\circ}\text{C}$ to $60\text{ }^{\circ}\text{C}$ is achieved using P and PID control algorithms.

For analysis, the open-loop and closed-loop results are presented in both the time and frequency domains.

2. Experimentation

The hand lay-up method was adopted to fabricate the glass-epoxy laminated composite beam by maintaining the weight fraction of 50:50. The Araldite LY-556 resin and HY-951 hardener were blended in a 10:1 ratio to prepare the epoxy resin. The petroleum jelly mold releasing agent was applied on the plastic sheet (OHP sheet) attached to the flat metallic base having a smooth surface. The gel coat is applied to the plastic sheet, which helps in protecting the fibers from environmental exposure. The bidirectional 280 GSM glass-fiber mats were laid one above the other to attain the desired thickness of the laminate. A sufficient quantity of resin mixture was used to make sure that the fiber mats were completely wet. The metallic rollers and the thick plastic strips were used to keep the laminates free from air entrapments. The fabricated laminates were cured for 24 hours in a pressure-controlled hydraulic press under 50 bar pressure at room temperature. The cured samples were then freed from the releasing plastic films, and the composite laminates were cut to 25 cm × 2.5 cm dimensions. The average thickness of the prepared samples was measured to be 0.25 cm.

2.1. Thermal Treatment of Laminated Composite Beam

The laminated composite beam specimens were thermally aged in the thermal environment. The thermal chamber is capable of conserving the desired temperature with a precision of less than ± 1 °C. The temperature profile was created to achieve a thermal environment ranging from -20 °C to 60 °C. At first, the temperature in the enclosure was decreased to -20 °C from the ambient temperature. The laminated composite beam is permitted to remain at -20 °C for 45 minutes. The free vibration tests were performed by creating an impulse signal of amplitude ± 5 volts and a period of 10 ms using the function generator. The PZT-5H sensor and actuation patches were used to obtain the frequency response plots. Then the temperature of the thermal chamber was increased to room temperature and sustained there for 30 minutes before getting the chamber to the next temperature. The temperature of the chamber was brought back to the reference temperature after performing a free vibration test at every elevated temperature value. Figure 1 shows the temperature profile at which the experiments were performed at different temperatures, i.e., -20 °C, 0 °C, 20 °C, 40 °C, 60 °C, and room temperature.

The desirable temperature profile was generated using the control panel and the

computer-assisted program, as shown in Figure 2. The temperature profile of 596 minutes (~10 hours) was controlled in the thermal chamber with a temperature deviation of less than ± 1 °C.

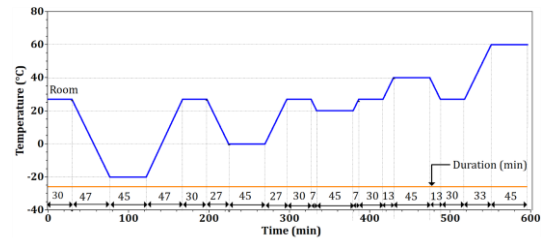


Fig. 1. Temperature profile generated to investigate the effect of temperature on AVC characteristics of a laminated composite cantilever beam for thermal chamber

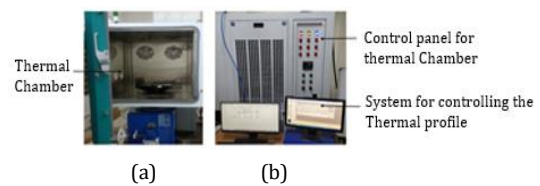


Fig. 2. Pictorial representation of the (a) thermal chamber and (b) temperature control unit.

2.2. Active Vibration Control

The glass-epoxy laminated composite beam specimen was fixed firmly in the cantilever position. Three PZT-5H piezoelectric patches of dimension 2 cm × 2 cm × 0.04 cm were mounted on the composite beam for actuation, sensing, and controlling actions. The actuator and controller patches were placed near the fixed end on the bottom and top of the composite beam, respectively. The sensing patch was positioned just beside the controlling patch on the composite beam. The pictorial representation of the patch position is presented in Figure 3 (a). The piezoelectric patches were attached to the beam using flex bond instant adhesive, and the surfaces of the patches were coated with the non-conductive PCB coating spray to protect the patches from moisture. The properties of the PZT-5H patch (Sparkler piezoceramics Pvt. Ltd., Pune) are presented in Table 1.

The sine signals were generated using the function generator connected to the actuating patch through the signal amplifier. The signals read from the sensing patch were amplified and fed to an analog input (AI) module (NI-DAQ 9234). The sensor signals were processed to compute the controlling signals. The computed controlling signals were sent to the controller patch through an analog output (AO) module (NI-DAQ 9263) and a signal amplifier. The AI and AO modules were loaded into the NI-CRIO-9053 data acquisition and a processing module. All the signals were acquired with a sampling rate of 25.6 kHz. The component connectivity diagram of the AVC system is presented in Figure 3 (b).

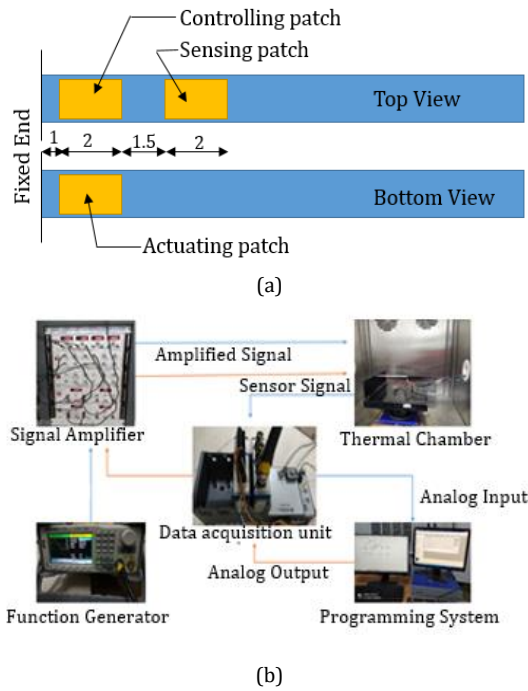


Fig. 3. Pictorial representation of (a) patch position (b) the active vibration control system in a thermal chamber with LabVIEW programming module

Table 1. The material properties of PZT-5H patches

| Properties | Magnitude |
|--------------------------------|--------------------------|
| Density (kg/m ³) | 7500 |
| Curie temperature (°C) | 190 |
| Piezoelectric charge constants | |
| d ₃₁ (C/N) | -265 × 10 ⁻¹² |
| d ₃₃ (C/N) | 550 × 10 ⁻¹² |
| Piezoelectric voltage constant | |
| g ₃₃ (Vm/N) | 19 × 10 ⁻³ |
| g ₃₁ (Vm/N) | -9 × 10 ⁻³ |

The signals acquired by the sensing module often get affected by disturbances. The faulty signals are made to pass through a physical filter module to eliminate the noise and disturbances. The band-pass filter was set to a range of 5 Hz to 50 Hz to avoid disturbances and restrict the study to only the fundamental vibration mode. The P and PID controllers were designed in the LabVIEW platform to attenuate the vibrating cantilever beam operating in elevated thermal environments. The code was developed in the LabVIEW programming environment to depict the control flowchart (i.e., Figure 5). The control gains were then set based on the engineering deduction. The controllers compute the required control signal amplitudes. The controlling signals are then passed on to the controller patch through the AO card and amplification module.

3. Validation Study

The behavior of the physical structures can be represented in terms of the mathematical expressions known as the plant models or the

transfer functions. The transfer functions are generated based on the outcome of the system for the given input signals. In this study, an impact hammer test was performed at room temperature to obtain the transfer function of the smart cantilever beam structure. The beam was excited by the impact hammer (PCB model: 086C03), and the vibration signals were acquired using the triaxial accelerometer (PCB model: 339A31/NC) mounted on the structure. The impact hammer and accelerometer signals were acquired using the AI card mounted (NI-DAQ 9234) on the USB chassis (NI-USB-9162). The acquired signals were used to obtain the frequency response functions (FRF) through the LabVIEW software module.

The system identification toolbox of the LabVIEW platform was used to obtain the transfer function of the laminated glass-epoxy composite cantilever beam. Experimentally obtained impact hammer signals and the accelerometer signals were used as input and output signals, respectively, to generate the transfer function of the system. The input and output signals collected for all the temperatures were then used to develop the transfer function of the model as represented by Eqn. 1. The second-order transfer function with two poles and two zeros was found to have an 86.27 % fit to the experimental results.

$$T_f = \frac{-0.4218 S^2 - 16.54 S - 2296}{S^2 + 17.86 S + 8.636 \times 10^4} \quad (1)$$

In order to further validate the obtained transfer function model, the simulation results were also compared with the experimentally obtained higher modes of vibrational frequencies. The actuator patch was excited with the power amplifier voltage of 70 RMS to excite the first four modes of vibrating the smart cantilever beam. The FRF curves plotted in Figure 4 indicate that the results obtained from the transfer function model excellently mimic the experimental or actual modal behavior of the structure.

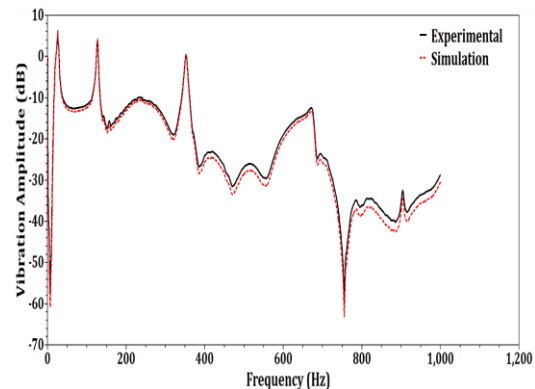


Fig. 4. Frequency response of the laminated composite beam operating at room temperature

The first four natural frequencies of the smart cantilever beam are presented in Table 2. From the results, it is evident that the simulation results are in good agreement with the experimental results. Additionally, the sensor voltages were also noted at the corresponding natural frequencies to appreciate the influence of the corresponding transverse deflections. The sensor voltage of 5.06 V is observed for the first mode of vibration, which is much higher compared to other vibratory modes. Hence, in this study, emphasis is given to controlling the first natural frequency of the laminated composite beam.

Table 2. The natural frequencies (in Hz) and corresponding sensor voltages of the smart cantilever beam

| Mode number | Natural frequency (Experimental) | Natural frequency (Simulation) | Sensor voltage (volts) |
|-------------|----------------------------------|--------------------------------|------------------------|
| 1 | 28.01 | 28.02 | 5.06 |
| 2 | 126.53 | 126.03 | 2.41 |
| 3 | 354.86 | 355.45 | 1.08 |
| 4 | 676.43 | 677.89 | 0.61 |

3.1. The Validation of the Controller Performance

The experimental vibration attenuation characteristics of the P and PID controllers were compared with the outcomes of the simulations. The MatLab Simulink module was used to obtain the simulation results of the AVC of the smart composite beam. Both the open-loop and the closed-loop model results are presented in order to appreciate the magnitude of vibration attenuation achieved. The open-loop and the closed-loop control algorithms used for the analysis are presented in Figure 5.

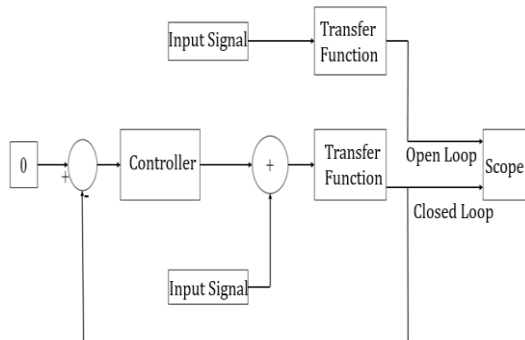


Fig. 5. Control algorithm adopted for P and PID controller

To validate the performance of the PID controller algorithm, the gains $K_p=0.09$, $T_i=8$, & $T_d=0.005$ were considered to perform the simulations and experimentations. The vibration attenuation performances of the PID controller obtained using simulations and experimentation are presented in Figure 6. The vibration

attenuation of 42.30 % and 43.10 % were achieved using experimental and numerical techniques, respectively. From the results, it is evident that the experimental and simulation results are in good agreement with each other.

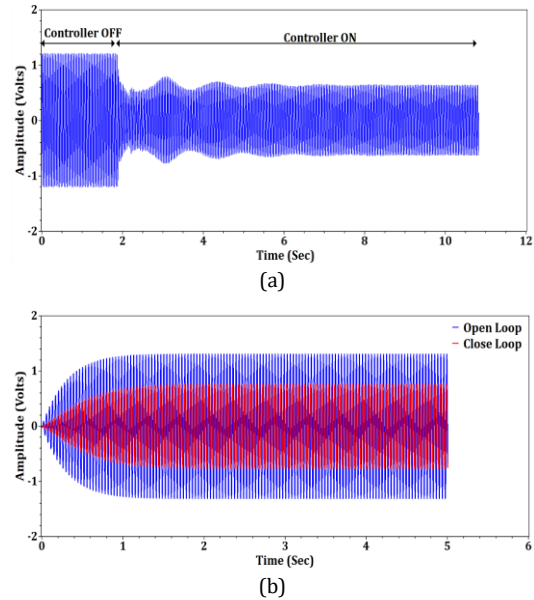


Fig. 6. Performance of the PID controller to attenuate the vibrating laminated composite cantilever beam operating at room temperature using (a) experimental and (b) simulation techniques

Similarly, the experimental results obtained from the P controller algorithm were also compared with the simulation results. The experimental and simulation results obtained with the proportional gain of $K_p = 0.9$ are presented in Figure 7. The vibration attenuation of 41.84 % and 42.90 % were accomplished using the experimental and simulations, respectively.

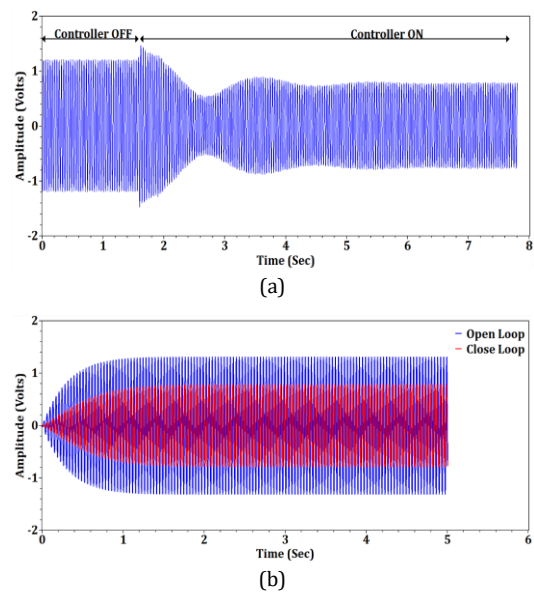


Fig. 7. Performance of the P controller to attenuate the vibrating laminated composite cantilever beam operating at room temperature using (a) experimental and (b) simulation techniques

4. Results and Discussion

The vibration attenuation capabilities of the developed P and PID control algorithms were investigated in elevated thermal environments. The temperatures ranging from -20 °C to 60 °C in the steps of 20 °C were considered for the investigation. For all the temperatures, the experiments were performed by considering the actuation RMS voltage of 12 V. The energy required for exciting the fundamental mode of the vibration is considerably lesser compared to the other modes of vibration. Hence, in this work, importance is given to attenuating the structure's fundamental mode of vibration. As noted earlier, the natural frequency of the glass-epoxy laminated composite beam is 28.01 Hz. Hence, the AVC performance was investigated up to 50 Hz.

The time-domain vibration attenuation performance of the developed P and PID control algorithms at -20 °C temperature are presented in Figure 8. A vibration reduction of 29.91 % and 19.09 % was observed for the PID and P controllers, respectively. It can be noted that the settling time for the P controller is considerably higher compared to the PID controller. The P controller algorithm reduces the steady-state error to keep the system in a stable state. However, in the presence of external disturbance, the difference between the desired and steady-state values never ceases to exist. This, in turn, causes the P control algorithm to take additional time to stabilize [19,27].

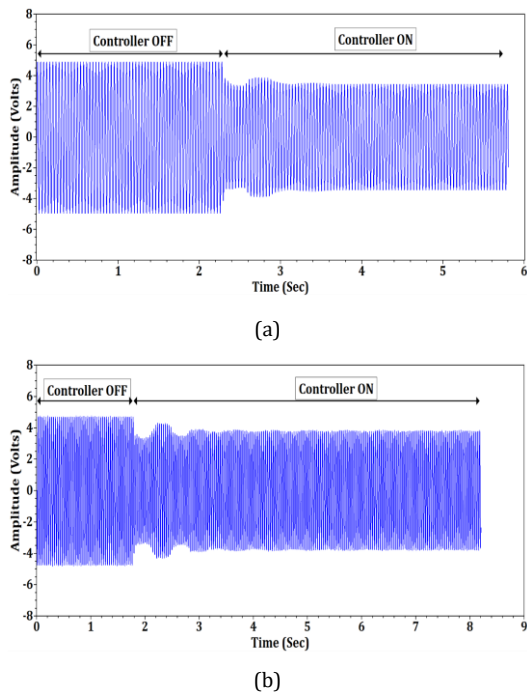


Fig. 8. The vibration attenuation results of the laminated composite beam operating in -20 °C thermal environment using the (a) PID controller and (b) P controller

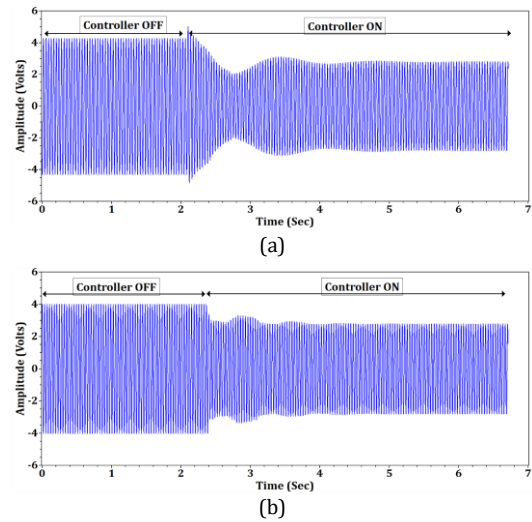


Fig. 9. The vibration attenuation results of the laminated composite beam operating in 0 °C thermal environment using the (a) PID controller and (b) P controller

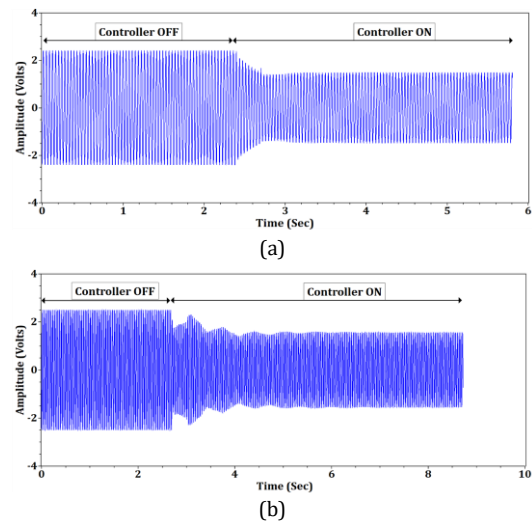


Fig. 10. The vibration attenuation results of the laminated composite beam operating in 20 °C thermal environment using the (a) PID controller and (b) P controller

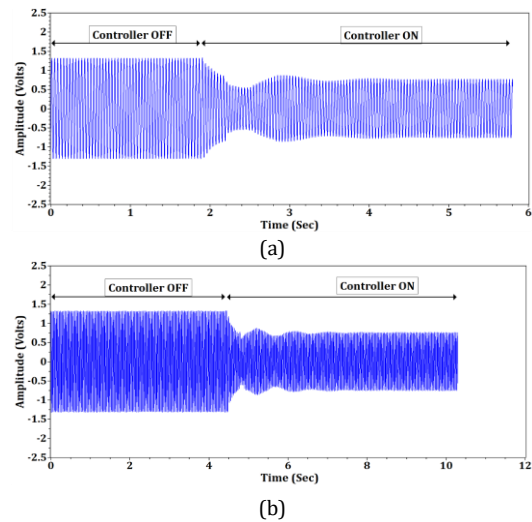


Fig. 11. The vibration attenuation results of the laminated composite beam operating in 28.5 °C thermal environment using the (a) PID controller and (b) P controller

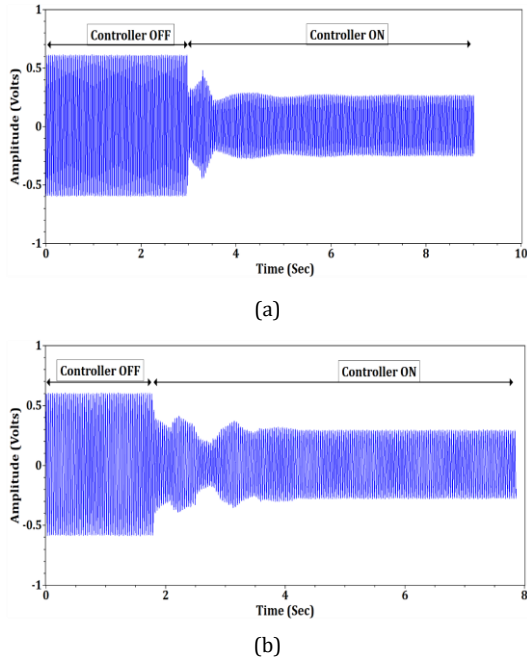


Fig. 12. The vibration attenuation results of the laminated composite beam operating in 40 °C thermal environment using the (a) PID controller and (b) P controller

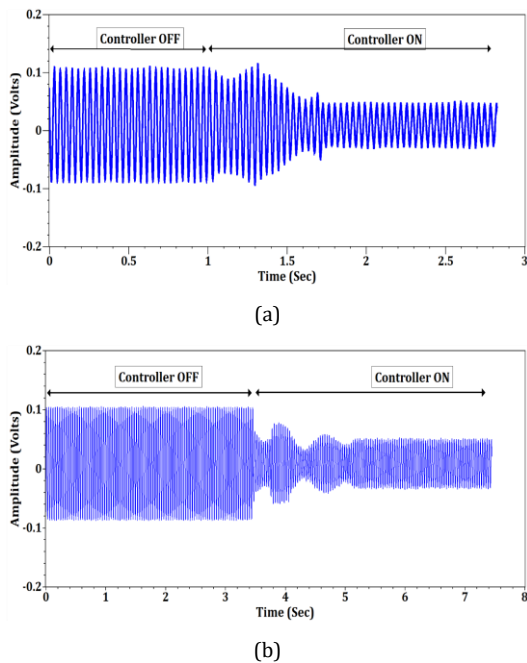


Fig. 13. The vibration attenuation results of the laminated composite beam operating in 60 °C thermal environment using the (a) PID controller and (b) P controller

Similarly, the AVC of the laminated composite beam was also achieved at 0 °C, 20 °C, 28.5 °C (room temperature), 40 °C, and 60 °C thermal environments. The vibration attenuation results obtained by P and PID controllers are presented in Figures 9 to 13. From the results, it is evident that the vibration attenuation characteristics of both P and PID controllers improved with an increase in temperature values. The improvement is primarily due to variations in the two essential process parameters. Firstly, with

the increase in the temperature, the AVC performance of the PZT-5H patch enhances considerably [28]. Specifically, the piezoelectric constant and the dielectric constant of the PZT-5H patch improve with an increase in temperature. Secondly, the stiffness of the structure considerably reduces with an increase in temperature. In the case of the laminated composite structures, the thermal properties of both constituent materials are considerably different; hence, on exposure to the thermal environment, both constituent materials behave differently. Hence, with the rise in temperature, the bond between the fiber and the matrix of the composite materials gets weak, as shown in Figure 14. This, in turn, reduces the strength and stiffness of the composite structure [29].

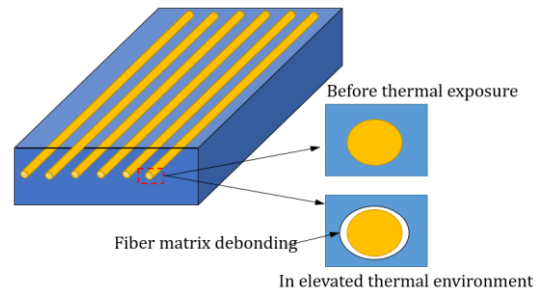


Fig. 14. Pictorial representation of fiber-matrix debonding of composite structures on exposure to the elevated thermal environments

From the results presented in Figures 9 to 13, it is apparent that the PID control algorithm provides better vibration attenuation compared to the P control algorithm. From results it was noted that, with the PID controller, the vibration attenuation of 29.91 %, 34.97 %, 38.64 %, 42.88 %, 58.4 %, and 60.39 % were achieved for -20 °C, 0 °C, 20 °C, 28.5 °C, 40 °C, and 60 °C temperatures, respectively. Similarly the vibration attenuation of 19.09%, 31.32 %, 38.50 %, 42.78 %, 52.04 %, and 53.92 % were noted for -20 °C, 0 °C, 20 °C, 28.5 °C, 40 °C, and 60 °C temperatures, respectively using the P control algorithm. The underperformance of the P controller is mainly due to its incapability to handle the steady state and transient errors.

The sensor output voltages were also recorded in controller off condition to appreciate the influence of temperature on the performance of the PZT-5H patch and are graphically represented in Figure 15. The results show that the sensor voltage output considerably reduces with an increase in temperature. This is primarily due to enhancement in vibration attenuation performance of the piezoelectric patches and reduction in stiffness of the host structure. The patch sensor voltage reduces from 4.88 volts to 0.101 volts for variation in temperature from -20 °C to 60 °C.

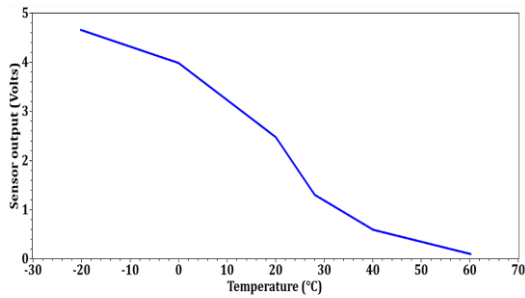


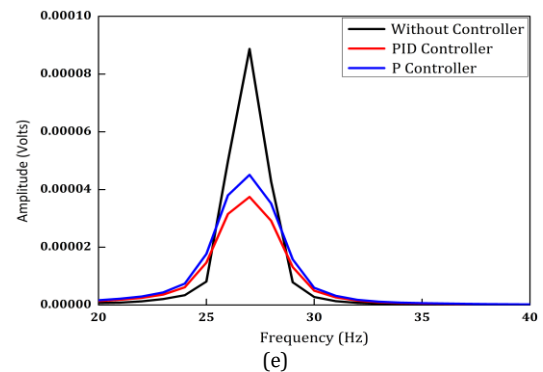
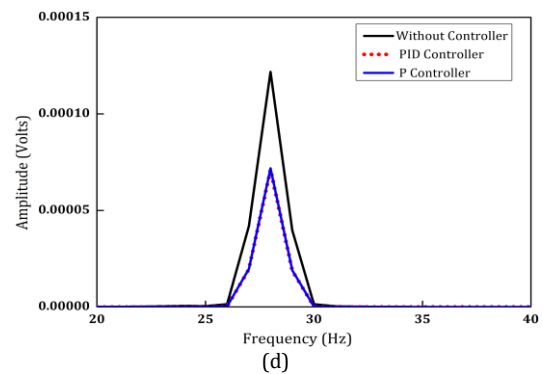
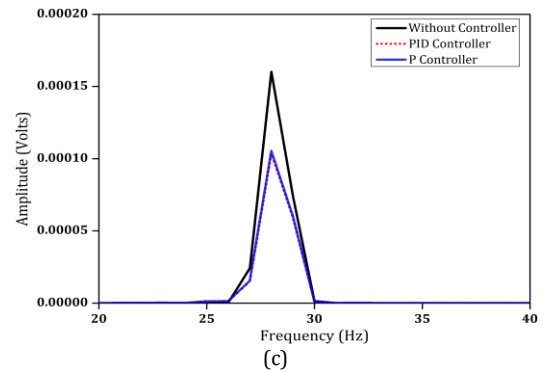
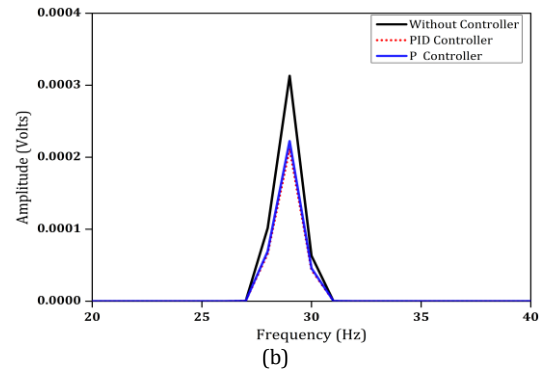
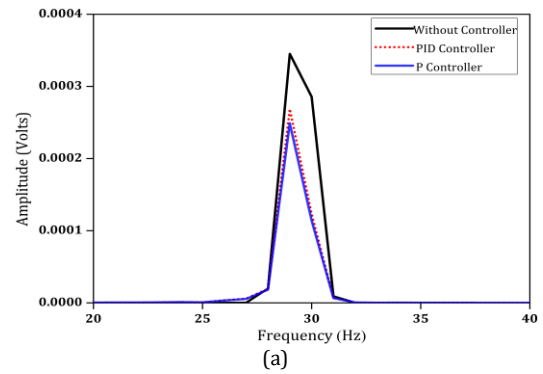
Fig. 15. Variation in the sensor output voltage of the laminated composite beam operating in various thermal environments

The controller parameters used to achieve the AVC of the cantilever glass-epoxy laminated composite beam are presented in Table 3. From the results, it can be noted the natural frequency of the system reduces continuously with an increase in temperature. The variation is mainly due to a reduction in stiffness of the system with an increase in temperature [30-33]. It can also be noted that the control voltage requirement also reduces with an increase in the magnitude of temperature.

The vibration attenuation performance of the P and PID control algorithms is also presented in the frequency domain in order to understand the influence of temperature on the natural frequency and amplitude of vibration. From the results presented in Figure 16, it is apparent that the system's natural frequency reduces with an increase in temperature. As observed in time domain plots, the frequency domain results also indicate an improvement in the performance of the vibration attenuation characteristics of the P and PID control algorithms. The amplitude of vibration reduction of 27.82 %, 32.36 %, 35.44 %, 40.75 %, 57.83 %, and 61.22 % were observed for PID controller operating in -20 °C, 0 °C, 20 °C, 28.5 °C, 40 °C, and 60 °C thermal environment respectively. Similarly, for P controller the reduction of 22.11 %, 28.97 %, 34.18 %, 40.16 %, 49.15 %, and 53.49 % were noted for -20 °C, 0 °C, 20 °C, 28.5 °C, 40 °C, and 60 °C temperatures respectively.

Table 3. The control voltage parameters used for AVC of the cantilever laminated composite beam operating in various temperature environments

| Temperature (°C) | Natural frequency (Hz) | Exiting voltage | Control voltage |
|------------------|------------------------|-----------------|-----------------|
| -20 | 29.75 | 12 | 8 |
| 0 | 28.98 | 12 | 8 |
| 20 | 28.08 | 12 | 7 |
| 28.5 | 28.82 | 12 | 7 |
| 40 | 26.98 | 12 | 6 |
| 60 | 24.92 | 12 | 5 |



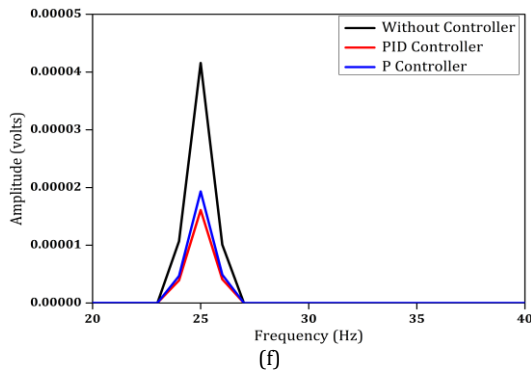


Fig. 16. The frequency response plots indicating the AVC of the cantilever laminated composite beam using P and PID controller at (a) $-20\text{ }^{\circ}\text{C}$, (b) $0\text{ }^{\circ}\text{C}$, (c) $20\text{ }^{\circ}\text{C}$, (d) $28.5\text{ }^{\circ}\text{C}$, (e) $40\text{ }^{\circ}\text{C}$, and (f) $60\text{ }^{\circ}\text{C}$

5. Conclusion

In this paper, the AVC of the cantilever glass-epoxy laminated composite beam is achieved using the amalgamation of the experimental and simulation methods. The performance of the P and PID control algorithms is investigated in various thermal environments ($-20\text{ }^{\circ}\text{C}$ to $60\text{ }^{\circ}\text{C}$). The simulation outcomes are correlated with the experimental results for verifications of the identified models. The effect of the temperature on the natural frequency, control algorithm performance, and peak amplitudes is investigated. Both the time domain and the frequency domain results are presented to appreciate the vibration attenuation achieved by the control algorithms. The amplitude of vibration reduction of 27.82 %, 32.36 %, 35.44 %, 40.75 %, 57.83 %, and 61.22 % were observed for PID controller operating in $-20\text{ }^{\circ}\text{C}$, $0\text{ }^{\circ}\text{C}$, $20\text{ }^{\circ}\text{C}$, $28.5\text{ }^{\circ}\text{C}$, $40\text{ }^{\circ}\text{C}$, and $60\text{ }^{\circ}\text{C}$ thermal environment respectively. Similarly, for P controller the reduction of 22.11 %, 28.97 %, 34.18 %, 40.16 %, 49.15 %, and 53.49 % were noted for $-20\text{ }^{\circ}\text{C}$, $0\text{ }^{\circ}\text{C}$, $20\text{ }^{\circ}\text{C}$, $28.5\text{ }^{\circ}\text{C}$, $40\text{ }^{\circ}\text{C}$, and $60\text{ }^{\circ}\text{C}$ temperatures, respectively. Additionally, the natural frequency of the system is reduced continuously with an increase in temperature.

Acknowledgments

The authors thank the Science and Engineering Research Board (**DST-SERB, Project No. EEQ/2017/000744**), Govt. of India, and Department of Mechanical Engineering, National Institute of Technology Karnataka Surathkal for providing all essential endowments and facilities to carry out this research.

References

- [1] J. Ye, 2003. Laminated Composite Plates and Shells. XIV, 274. <https://doi.org/10.1007/978-1-4471-0095-9>.
- [2] A. Garg and H. D. Chalak, 2019. A review on analysis of laminated composite and sandwich structures under hygrothermal conditions. *Thin-Walled Struct.*, vol. 142, no., pp. 205–226. <https://doi.org/10.1016/j.tws.2019.05.005>.
- [3] V. Kallannavar and S. Kattimani, 2021. Effect of temperature on the performance of active constrained layer damping of skew sandwich plate with CNT reinforced composite core. *Mech. Adv. Mater. Struct.*, vol. 0, no. 0, pp. 1–20. <https://doi.org/10.1080/15376494.2021.1955315>.
- [4] T. Bailey and J. E. Ubbard, 1985. Distributed piezoelectric-polymer active vibration control of a cantilever beam. *J. Guid. Control. Dyn.*, vol. 8, no. 5, pp. 605–611. <https://doi.org/10.2514/3.20029>.
- [5] M. Biswal, S. K. Sahu, and A. V. Asha, 2015. Experimental and numerical studies on free vibration of laminated composite shallow shells in hygrothermal environment. *Compos. Struct.*, vol. 127, pp. 165–174. <https://doi.org/10.1016/j.compstruct.2015.03.007>.
- [6] H. S. Panda, S. K. Sahu, and P. K. Parhi, 2013. Hygrothermal effects on free vibration of delaminated woven fiber composite plates - Numerical and experimental results. *Compos. Struct.*, vol. 96, pp. 502–513. <https://doi.org/10.1016/j.compstruct.2012.08.057>.
- [7] S. Fazeli, C. Stokes-Griffin, J. Gilbert, and P. Compston, 2020. An analytical solution for the vibrational response of stepped smart cross-ply laminated composite beams with experimental validation. *Compos. Struct.*, vol. 266, no., pp. 1–10. <https://doi.org/10.1016/j.compstruct.2021.113823>.
- [8] A. P. Parameswaran, A. B. Pai, P. K. Tripathi, and K. V. Gangadharan, 2013. Active vibration control of a smart cantilever beam on general purpose operating system. *Def. Sci. J.*, vol. 63, no. 4, pp. 413–417. <https://doi.org/10.14429/dsj.63.4865>.
- [9] R. Rimašauskienė, V. Jūrėnas, M. Radzienski, M. Rimašauskas, and W. Ostachowicz, 2019. Experimental analysis of active-passive vibration control on thin-walled composite beam. *Compos. Struct.*, vol. 223, no. <https://doi.org/10.1016/j.compstruct.2019.110975>.
- [10] Y. Li, X. Wang, R. Huang, and Z. Qiu, 2015. Active vibration and noise control of vibro-

- acoustic system by using PID controller. *J. Sound Vib.*, vol. 348, pp. 57–70. <https://doi.org/10.1016/j.jsv.2015.03.017>.
- [11] S. Zhang, R. Schmidt, and X. Qin, 2015. Active vibration control of piezoelectric bonded smart structures using PID algorithm. *Chinese J. Aeronaut.*, vol. 28, no. 1, pp. 305–313. <https://doi.org/10.1016/j.cja.2014.12.005>.
- [12] A. M. Simonović, M. M. Jovanović, N. S. Lukić, N. D. Zorić, S. N. Stupar, and S. S. Ilić, 2016. Experimental studies on active vibration control of smart plate using a modified PID controller with optimal orientation of piezoelectric actuator. *JVC/Journal Vib. Control*, vol. 22, no. 11, pp. 2619–2631. <https://doi.org/10.1177/1077546314549037>.
- [13] A. P. Parameswaran and K. Gangadharan, 2015. Parametric modeling and FPGA based real time active vibration control of a piezoelectric laminate cantilever beam at resonance. *JVC/Journal Vib. Control*, vol. 21, no. 14, pp. 2881–2895. <https://doi.org/10.1177/1077546313518818>.
- [14] A. P. Parameswaran, B. Ananthakrishnan, and K. V. Gangadharan, 2015. Design and development of a model free robust controller for active control of dominant flexural modes of vibrations in a smart system. *J. Sound Vib.*, vol. 355, pp. 1–18. <https://doi.org/10.1016/j.jsv.2015.05.006>.
- [15] M. A. Kamel, K. Ibrahim, and A. E. Ahmed, 2019. Vibration control of smart cantilever beam using finite element method. *Alexandria Eng. J.*, vol. 58, no. 2, pp. 591–601. <https://doi.org/10.1016/j.aej.2019.05.009>.
- [16] A. Sharma, R. Kumar, R. Vaish, and V. S. Chauhan, 2016. Experimental and numerical investigation of active vibration control over wide range of operating temperature. *J. Intell. Mater. Syst. Struct.*, vol. 27, no. 13, pp. 1846–1860. <https://doi.org/10.1177/1045389X15615968>.
- [17] A. Sharma, R. Kumar, R. Vaish, and V. S. Chauhan, 2015. Active vibration control of space antenna reflector over wide temperature range. *Compos. Struct.*, vol. 128, pp. 291–304. <https://doi.org/10.1016/j.compstruct.2015.03.062>.
- [18] A. Sharma, A. Kumar, C. K. Susheel, and R. Kumar, 2016. Smart damping of functionally graded nanotube reinforced composite rectangular plates. *Compos. Struct.*, vol. 155, pp. 29–44. <https://doi.org/10.1016/j.compstruct.2016.07.079>.
- [19] V. Gupta, M. Sharma, N. Thakur, and S. P. Singh, 2011. Active vibration control of a smart plate using a piezoelectric sensor-actuator pair at elevated temperatures. *Smart Mater. Struct.*, vol. 20, no. 10. <https://doi.org/10.1088/0964-1726/20/10/105023>.
- [20] Mohammadrezazadeh S, Jafari AA., 2020. Active control of free and forced vibration of rotating laminated composite cylindrical shells embedded with magnetostrictive layers based on classical shell theory. *Mech Adv Compos Struct* 2020;7:355–69. <https://doi.org/10.22075/MACS.2020.16921.1191>.
- [21] Mohammadrezazadeh S, Jafari AA., 2021. Nonlinear vibration suppression of laminated composite conical shells on elastic foundations with magnetostrictive layers. *Compos Struct.*, 258:113323. <https://doi.org/10.1016/j.compstruct.2020.113323>.
- [22] Mohammadrezazadeh S., 2022. Vibration suppression of truncated conical shells embedded with magnetostrictive layers based on first order shear deformation theory. *J Theor Appl Mech.* <https://doi.org/10.15632/jtam-pl/112419>.
- [23] Mohammadrezazadeh S, Jafari AA., 2021. Nonlinear vibration analysis of laminated composite angle-ply cylindrical and conical shells. *Compos Struct* 2021;255:112867. <https://doi.org/10.1016/j.compstruct.2020.112867>.
- [24] Mohammadrezazadeh S, Jafari AA., 2019. The influences of magnetostrictive layers on active vibration control of laminated composite rotating cylindrical shells based on first-order shear deformation theory. *Proc IMechE Part C J Mech Eng Sci*;0:1–14. <https://doi.org/10.1177/0954406219830439>.
- [25] Mohammadrezazadeh S, Jafari AA., 2022. Active control of free and forced vibration of rotating laminated composite cylindrical shells embedded with magnetostrictive layers based on classical shell theory. *Mech Adv Compos Struct.* <https://doi.org/10.22075/MACS.2020.16921.1191>.
- [26] Mohammadrezazadeh S, Jafari AA., 2022. Vibration control of laminated truncated

- conical shell via magnetostrictive layers. *Mech Adv Mater Struct.*, 27:1756–64. <https://doi.org/10.1080/15376494.2018.1525627>.
- [27] Y. O. Lee, C. W. Lee, C. C. Chung, Y. Son, P. Yoon, and I. Hwang, 2008. Stability Analysis of an Electric Parking Brake (EPB) System with a Nonlinear Proportional Controller. vol. 41, no. 2. IFAC, 2008.
- [28] D. Wang, Y. Fotinich, and G. P. Carman, 1998. Influence of temperature on the electromechanical and fatigue behavior of piezoelectric ceramics. *J. Appl. Phys.*, vol. 83, no. 10, pp. 5342–5350. <https://doi.org/10.1063/1.367362>.
- [29] M. Rezaei, V. Karatzas, C. Berggreen, and L. A. Carlsson, 2020. The effect of elevated temperature on the mechanical properties and failure modes of GFRP face sheets and PET foam cored sandwich beams. *J. Sandw. Struct. Mater.*, vol. 22, no. 4, pp. 1235–1255. <https://doi.org/10.1177/1099636218781995>.
- [30] V. Kallannavar, S. Kattimani, M. E. M. Soudagar, M. A. Mujtaba, S. Alshahrani, and M. Imran, 2021. Neural network-based prediction model to investigate the influence of temperature and moisture on vibration characteristics of skew laminated composite sandwich plates. *Materials (Basel)*, vol. 14, no. 12. <https://doi.org/10.3390/ma14123170>.
- [31] V. Kallannavar, Balaji Kumaran, S. Kattimani, 2020. Effect of temperature and moisture on free vibration characteristics of skew laminated hybrid composite and sandwich plates. *Thin-Walled Structures*, 157, 107113. <https://doi.org/10.1016/j.tws.2020.107113>.
- [32] V. Kallannavar, S. Kattimani, H. Ramesh, "Influence of Temperature and Moisture on Free Vibration Behavior of Skew Laminated Composite Sandwich Panels with CNTRC Core," *International Journal of Structural Stability and Dynamics* (2022): 2250083. <https://doi.org/10.1142/S0219455422500833>
- [33] A. Ravi Kiran, V. Kallannavar, S. Kattimani, 2022. Vibration control of laminated composite cantilever beam operating in elevated thermal environments using fuzzy logic controller. *Noise & Vibration Worldwide*. 09574565221093240. <https://doi.org/10.1177/09574565221093240>.

